Conference Paper, Published Version

Sassa, Shinji

Depth of Mobile Layer under Severe Wave Conditions: Liquefaction Effect

Depth of Mobile Layer Under Severe Wave Conditions: Liquefaction Effect

By

Shinji Sassa

Research Fellow of the Japan Society for the Promotion of Science, Disaster Prevention Research Institute, Kyoto University, Kyoto 611-0011, Japan,(sassa@kaigan.dpri.kyoto-u.ac.jp).

ABSTRACT The wave-induced build-up of pore water pressures that occurs primarily under wave pressure fluctuation rather than oscillatory flow, is shown here to play a vital role in causing transport of fine sediments under waves. Poro-elastic analysis is presented on the depth of mobile layer under waves, and the results are compared with the existing theory in oscillatory flow. The effect of the oscillatory change in effective stress is identified that may manifest itself under severe wave conditions. For soft fine sediments, however, wave-induced liquefaction or fluidization resulting in the complete loss of effective stresses can take place. The simultaneous processes of the wave-induced liquefaction and sediment transport are reproduced here by the poro-elastoplastic finite element analyses. It is found that the thickness of mobile layer can develop rapidly in loose beds of fine sand or silt owing to the build-up of residual pore pressures, under severe yet considerably lower levels of wave loading than in the situation where only oscillatory flow effect is considered.

INTRODUCTION

The depth in which sediment becomes mobile under waves is one of the most fundamental questions in modelling the coastal sediment transport processes. When sediment becomes mobile, the following relation has been assumed to hold at the bottom of the mobile layer (Nielsen, 1992):

$$|\tau_{zx}| = K\sigma'_{z0} \tag{1}$$

where τ_{zx} is a horizontal shear stress, σ'_{z0} is an initial vertical effective stress and K represents a friction coefficient of soil skeleton. The shear stress changes due to the wave-induced oscillatory flow have been well described based on the knowledge of fluid mechanics. However, the changes in effective stresses due to the presence of oscillatory and residual pore pressures in the soil, as shown in Fig. 4 of the present

paper, were out of the scope of fluid mechanics. The integrated use of soil mechanics and fluid mechanics is thus vital for a rational understanding of the wave-induced sediment transport processes.

The paper is aimed at clarifying the role of the build-up of pore water pressures in causing sediment transport under waves. The theoretical background to represent the severity of wave loading will be described first. Then, the paper presents poro-elastic and elastoplastic analyses on the thickness of mobile layer under waves.

REPRESENTATION OF THE SEVERITY OF WAVE LOADING

The passage of wave trains exert two forms of action on the soil surface, namely, wave pressure fluctuation and oscillatory flow, both of which should induce horizontal shear stress in the soil.

The severity of the wave pressure fluctuation on a given horizon of soil may be expressed in terms of the cyclic stress ratio $\chi \equiv \tau / \sigma'_{v0}$ where τ represents the wave-induced maximum shear stress at that horizon and σ'_{v0} the initial vertical effective stress there. With the aid of a poro-elasticity theory (Madsen,1978; Yamamoto et al., 1978), the cyclic stress ratio at the level of the soil surface reduces to the following dimensionless parameter (Sassa and Sekiguchi, 1999)

$$\chi_0 \equiv \left[\frac{\tau}{\sigma'_{v0}}\right]_{z=0} = \frac{\kappa u_0}{\gamma'} \tag{2}$$

where u_0 is the amplitude of the wave-induced pressure fluctuation on the soil surface, κ is the wave number defined by $2\pi/L$ and γ' is the submerged unit weight of soil defined by $(\rho_s - \rho)g/(1+e)$. Here ρ_s is the density of soil particle, ρ is the density of fluid, g is the acceleration due to gravity and e is the void ratio of the soil.

The severity of the wave-induced oscillatory flow may be expressed by the dimensionless parameter S which represents the ratio of inertial to gravity forces acting on individual grains of soil (Sleath, 1994):

$$S = \frac{\rho U_0 \omega}{(\rho_s - \rho)g} \tag{3}$$

where U_0 is the velocity amplitude of the wave-induced oscillatory flow on the soil surface and ω is the angular wave frequency defined by $2\pi/T$.

On the basis of the linear wave theory where $U_0 = \kappa u_0 / (\rho\omega)$, I obtain the following relationship:

$$\chi_0 = S(1+e) \tag{4}$$

Thus, the severity of wave loading can be represented by either χ_0 or S. In the sections that follow, the parameter S will be used to discuss the thickness of mobile layer under waves.

PORO-ELASTIC ANALYSIS AND DISCUSSION

Suppose that small-amplitude sinusoidal fluid wave trains with a wave number κ and an angular wave frequency ω propagate over a plane bed, inducing on the seabed surface both the fluid pressure fluctuation having a pressure amplitude u_0 and the oscillatory flow having a velocity amplitude U_0. The boundary conditions on the soil surface can then be expressed as follows.

$$\begin{aligned} &\tilde{u}_0 = u_0 \cos(\kappa x - \omega t) \\ &\sigma_z = \tilde{u}_0 \\ &\tau_{zx}^{(1)} = \frac{1}{2}\rho f_\omega U_0^{\,2} \cos(\kappa x - \omega t - \phi) \\ &\text{on} \quad z = 0 \end{aligned} \tag{5}$$

where $\tau_{zx}^{(1)}$ is the oscillatory flow-induced shear stress with a phase lead ϕ and f_w is a friction factor defined by Jonsson(1963).

The wave pressure fluctuation $\tilde{u}_0$ which corresponds to the total stress change σ_z is important since it causes changes in stress state in the soil domain ($z \leqq 0$). With the aid of a poro-elasticity theory (Madsen, 1978; Yamamoto et al., 1978), it follows that

$$\tau_{zx}^{(2)} = -u_0 \kappa z \exp(\kappa z) \sin(\kappa x - \omega t) \tag{6}$$

$$\Delta\sigma'_z = -u_0 \kappa z \exp(\kappa z) \cos(\kappa x - \omega t) \tag{7}$$

where $\tau_{zx}^{(2)}$ is the pressure fluctuation-induced horizontal shear stress at a soil depth z and $\Delta\sigma'_z$ is the change in the vertical effective stress at this location z.

The oscillatory flow-induced shear stress $\tau_{zx}^{(1)}$ defined in Eq. (5) is assumed here to hold its value at the shallow depth z. The wave-induced horizontal shear stress τ_{zx} at the location z may then be expressed as $\tau_{zx} = \tau_{zx}^{(1)} + \tau_{zx}^{(2)}$. Let us now consider the sediment mobility on the basis of the relationship $|\tau_{zx}| = K\sigma'_z$. From Eqs. (5) to (7), it

follows at a generic point x=0 that

$$\left|0.5\rho f_w U_0^2 \cos(\omega t+\phi)+\kappa u_0 z\exp(\kappa z)\sin(\omega t)\right| = K\left(-\frac{\rho_s-\rho}{1+e}gz-\kappa u_0 z\exp(\kappa z)\cos(\omega t)\right) \quad (8)$$

Representing the pressure amplitude $u_0 = \rho U_0 \omega/\kappa$ and the mobile layer thickness δ = -z in Eq. (8), I obtain the following form:

$$S^2\left[\left(\frac{\delta}{af_w\exp(\kappa\delta)}\right)^2+0.25+\frac{\delta}{af_w\exp(\kappa\delta)}\sin(\phi)\right]\cos^2(\omega t+\theta) = \left(\frac{K}{1+e}\right)^2\left(\frac{\delta}{af_w}\right)^2\left(1+\frac{S(1+e)\cos(\omega t)}{\exp(\kappa\delta)}\right)^2 \quad (9)$$

where a = U_0/ω is the fluid particle semi-excursion, $\kappa\delta = \kappa af_w \times \delta/af_w$ and

$$\tan(\theta)=\tan(\phi)+\frac{2}{\cos(\phi)}\frac{\delta}{af_w\exp(\kappa\delta)} \qquad 0\le\theta\le\pi/2 \quad (10)$$

Eq. (9) can make it possible to predict the variation of the depth of the mobile layer with time in the course of a given wave cycle.

An example calculation using Eq. (9) is shown in Fig. 1. The parameters used, $K/(1+e)=1/3$ and $\phi = 22.5^\circ$, are the same as those used by Zara Flores and Sleath (1998). The predicted form of variation is not sinusoidal, and is consistent with the measurements in oscillatory flow (Zala Flores and Sleath, 1998). The maximum thickness of the mobile layer, δ_{max}, under waves, manifest itself at a particular phase namely near trough of the waves.

The predicted variations of δ_{max} against *S* are plotted in Fig. 2 with solid curves for four different values of $\kappa a f_w$. For the purpose of comparison, a theoretical curve developed by Sleath (1994) for a pure oscillatory flow is also plotted in this figure with the dotted curve. The Sleath-curve was shown to conform with the measurements in Zara Fores and Sleath(1998). The present results fall on a single straight line for low values of *S*. This implies that there is a linear relation between the mobile layer thickness as defined by δ_{max}/D and the Shields parameter $0.5\rho f_w U_0^2/(\rho_s-\rho)gD$, which is in accordance with the previous results by several other investigators (e.g., Asano, 1993).

But, the value of δ_{max} develops rapidly for high values of *S*, depending strongly on the parameter $\kappa a f_w$. A difference can be seen between the present results for $\kappa a f_w = 0$ and the Sleath theoretical curve for A=0. This may represent the effect of the fluctuation in the vertical effective stress under waves. In fact, the threshold value of *S* at which the δ_{max} / af_w-value increases rapidly, decreases from 0.3 for pure oscillatory flow to 0.25 for waves.

The poro-elastic analysis as described above should correspond to the behaviour of dense and coarse sand in the sense that only oscillatory pore pressures are present in the soil. The next section will clarify the effect of the residual pore pressures in fine sediments on the basis of the poro-elastoplastic finite element analyses.

ELASTO-PLASTIC FINITE ELEMENT ANALYSES

Under severe wave conditions, wave-induced liquefaction due to the build-up of residual pore pressures should occur owing to the cyclic plasticity nature (contractive behaviour) of cohesionless soil. The poro-elastoplastic finite element analysis developed by Sassa and Sekiguchi (2001) can describe the changes in shear stress and effective stresses in the course of the liquefaction. The present study extends the analysis so as to consider the shear stress due to oscillatory flow under waves.

Two sets of the finite element analysis were performed for a total of 15 cycles of wave loading in each set, with the aim of reproducing the observed wave-induced liquefaction in loose beds of silt (mean grain diameter $D_{50} = 0.05mm$) and fine sand ($D_{50} = 0.15mm$). The wave loading and the geometry are shown for each set in Fig.3. It is important here to note that the partial drainage factor Φ (Sassa and Sekiguchi, 1999) is defined by

$$\Phi = \frac{k_D}{m_v \gamma_f \omega} \kappa^2 \tag{11}$$

where k_D is the Darcy coefficient of permeability of the soil, $\gamma_f = \rho g$ is the unit weight of the fluid and m_v is the coefficient of compressibility of the soil skeleton. The Φ-value for the loose fine sand was equal to 4.7×10^{-3}, which was significantly higher than 1.8×10^{-6} for the loose silt. The values of the parameter $\kappa a f_w$ were 0.001 and 0.002 respectively. These parameters were determined with reference to the wave and soil conditions imposed in the experiments by Sassa and Sekiguchi (1999) and Foda and Tzang (1994). The friction factor f_w was calculated from Jonsson's (1963) formula

with a roughness height equal to $2D_{50}$.

A typical set of the results on the variations of stresses at the bottom of the mobile layer is shown in Fig. 4. The fluctuation in the horizontal shear stress τ_{vh} remain unchanged during the first 12 cycles or so, while the vertical effective stress σ'_v decreases continuously owing to the build-up of residual pore pressure $u_e^{(2)}$ in the soil. At the 15th wave loading cycle, liquefaction takes place such that $u_e^{(2)} \cong \sigma'_{v0}$, allowing the sediment to become mobile at this soil depth according to the relationship $|\tau_{vh}| = K\sigma'_v$.

The influence of the severity of wave loading on the development of the liquefaction can be clearly seen in the form of Fig. 5. The wave-induced changes in both the residual pore pressure ratio $u^{(2)}_e/\sigma'_{v0}$ and the effective stress ratio p^*/σ'_v are plotted against the cyclic stress ratio χ_0. For the purpose of discussion, the soil responses to wave pressure fluctuation, namely without the oscillatory flow-induced shear stress, are also plotted in Fig. 5. The results indicate that there exists a critical cyclic stress ratio χ_{cr} below which liquefaction does not occur. It is also noteworthy that there is no significant difference between the results under wave pressure fluctuation and under waves which involve both wave pressure fluctuation and oscillator flow. The wave pressure fluctuation, rather than oscillatory flow, may thus be responsible for the occurrence of the wave-induced liquefaction.

The results of the elastoplastic analysis are superimposed on the results of the elastic analysis, giving a summary plot as shown in Fig. 6. Note here that the elastic response represents the absence of residual pore pressures with only oscillatory pore pressures involved, which may correspond to high values of Φ for dense and coarse sand. For the loose fine sand with $\Phi = 4.7 \times 10^{-3}$ in Fig. 6, however, the δ_{max}-value develops more rapidly owing to the build-up of residual pore pressures in the soil. The liquefaction effect is further significant for the loose silt with $\Phi = 1.8 \times 10^{-6}$.

Verification of the Predicted Depth of Mobile Layer with the Measurements of Wave-Induced Liquefaction

Sassa and Sekiguchi (1999) performed a series of centrifuge wave tank tests on loose beds of fine sand (mean grain size $D_{50} = 0.15mm$) with viscous scaling introduced, such that time scaling laws for wave propagation as well as consolidation of soil were

matched. The critical cyclic stress ratio χ_{cr} for liquefaction to occur was found to be 0.14, in accordance with the predictions as shown in Fig 5. This value corresponds to $S = 0.075$ on the basis of the relationship $S = \chi_0/(1+e)$. The measured thickness of liquefied zone for the threshold value of S is plotted in Fig. 6. The measured thickness of $\delta_{max}/af_w = 256$ is consistent with the predicted thickness of $\delta_{max}/af_w = 148$.

Foda and Tzang (1994) performed a series of wave flume tests on loose beds of silt ($D_{50} = 0.05mm$) and sand ($D_{50} = 0.29mm$). They observed the occurrence of liquefaction due to the build-up of residual pore pressures in silt. I calculated the S-values for their data and found that liquefaction took place at the value of S as low as 0.03. In contrast, no significant residual pore pressures or sediment transport took place for sand, owing to the high value of Φ. The both measured results for silt and sand conform well with the predictions shown in Fig. 6.

The results described above demonstrate that the poro-elastoplastic finite element analysis combined with the fluid mechanics approach for describing the oscillatory flow-induced shear stresses can predict consistently the maximum thickness of the mobile layer under given wave and soil conditions, emphasizing the effect of the wave-induced liquefaction in beds of silt or fine sand.

CONCLUSIONS

The thickness of mobile layer under waves has been discussed on the basis of poro-elastic and elastoplastic analyses, with the aim of demonstrating the effect of the wave-induced build-up of pore water pressures. It is found that there are three important dimensionless parameters: the wave severity parameter S or χ_0, the partial drainage factor Φ and the newly defined wave friction parameter κaf_w. When the κaf_w-value is low, there could occur a rapid increase in the normalized maximum mobile layer thickness $\delta_{max}/af_{w.}$ The threshold wave condition, namely the critical S-value, depends on the magnitude of Φ for a given sediment. For dense and coarse sediments with high values of Φ, the predicted critical S-value is equal to 0.25 which is slightly lower than the value of 0.3 in pure oscillatory flow. The difference represents the effect of the fluctuating vertical effective stress under waves. The situation changes remarkably when dealing with loose fine sediments with low values of Φ. In fact, the critical S-value reduces to as low as 0.06 for loose beds of fine-grained sand and further to 0.03

for silt, owing to the wave-induced build-up of residual pore water pressures. The wave pressure fluctuation, not oscillatory flow, is responsible for the rapid increase in mobile layer thickness in the fine sediments.

REFERENCES

1. Asano, T., 1993, "Observations of granular-fluid mixture under an oscillatory sheet flow", *Proc. 22th Int. Conf. Coastal Eng., ASCE,* Reston, 1896-1909.
2. Foda, M.A. and S.-Y. Tzang, 1994, "Resonant fluidization of silty soil by water waves", *J. Geophys. Res. 99* (C10), 20,463--20,475.
3. Jonsson, I.G., 1963, "Measurements in the turbulent wave boundary layer", *Proc. 10th Congress IAHR*, London, 85-92.
4. Madsen, O.S., 1978, "Wave-induced pore pressures and effective stresses in a porous bed", *Géotechnique 28* (4), 377-393.
5. Nielsen, P., 1992, "*Coastal bottom boundary layers and sediment transport",* World Scientific, Singapore, pp 324.
6. Sassa, S. and H. Sekiguchi, 1999, "Wave-induced liquefaction of beds of sand in a centrifuge", *Géotechnique 49* (5), 621-638.
7. Sassa, S. and H. Sekiguchi, 2001, "Analysis of wave-induced liquefaction of sand beds", *Géotechnique 51* (2), 115-126.
8. Sleath, J.F.A., 1994, "Sediment transport in oscillatory flow", in *Sediment Transport Mechanisms in Coastal Environments and Rivers* edited by M. Belorgey, R.D.Rajaona and J.F.A. Sleath, World Scientific, Singapore.
9. Yamamoto, T., H.L. Koning., H. Sellmeijer. and E. Hijum, 1978, "On the response of a poro-elastic bed to water waves", *J. Fluid Mech*. *87*, 193-206.
10. Zala Flores, N. and J.F.A. Sleath, 1998, "Mobile layer in oscillatory sheet flow", *J. Geophys. Res. 103*, C6, 12,783-12,786.

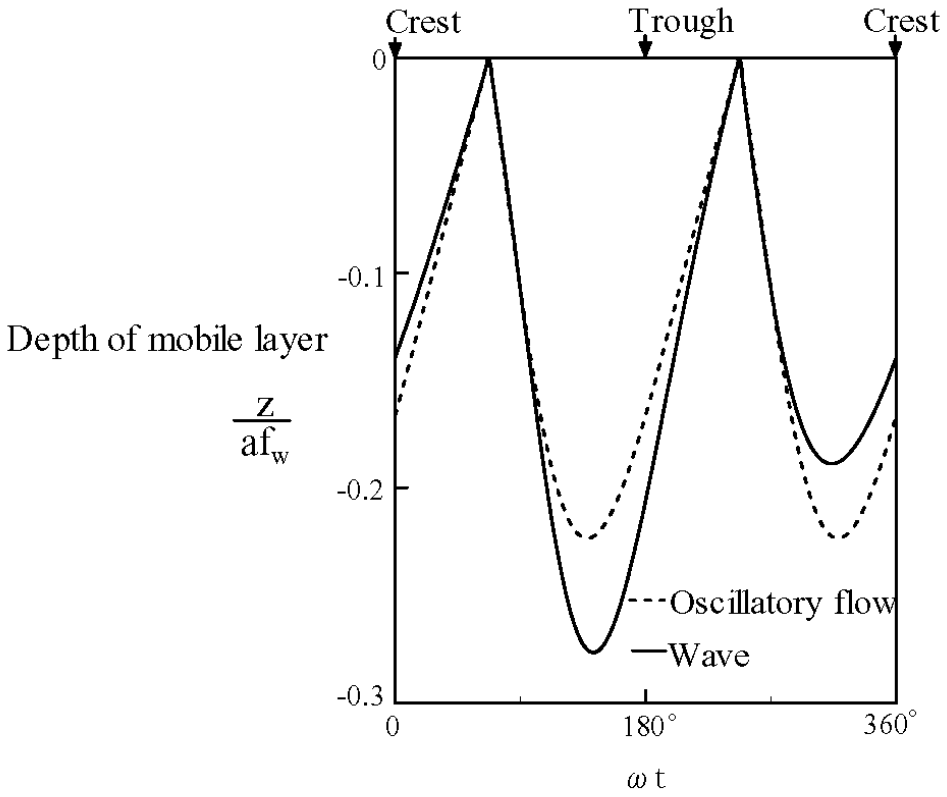

a: Fluid particle semi-excursion U_0 / ω

f_w: Jonsson's friction factor $2 \tau_0 / (\rho U_0^2)$

Fig.1 — Variation of the depth of the mobile layer with time during a wave cycle (S= 0.12, Φ=22.5°, e= 0.6, K=0.53)

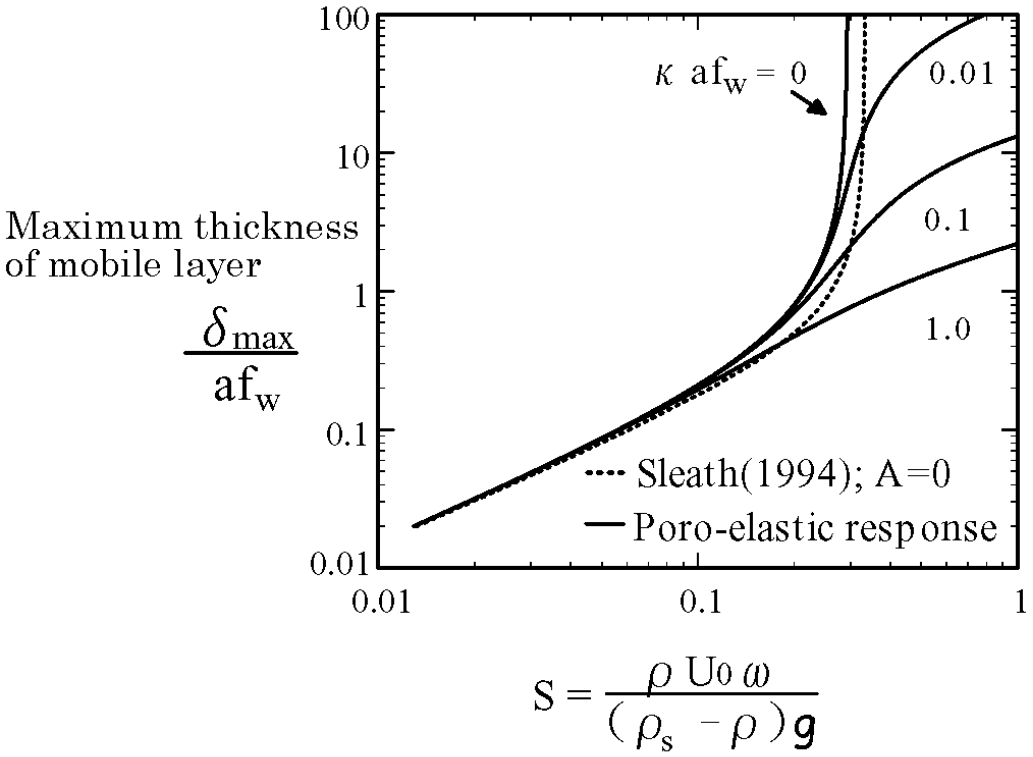

Fig.2 — Variation of normalized maximum mobile-layer thickness with S during a wave cycle

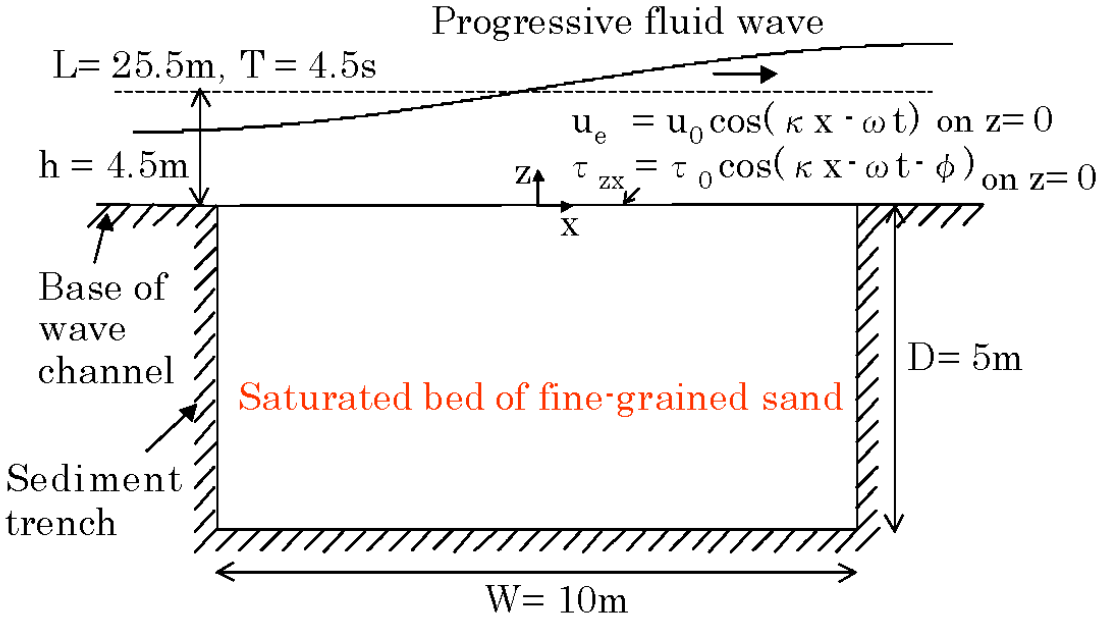

(a) Proto-type for the centrifuge model by Sassa and Sekiguchi(1999)

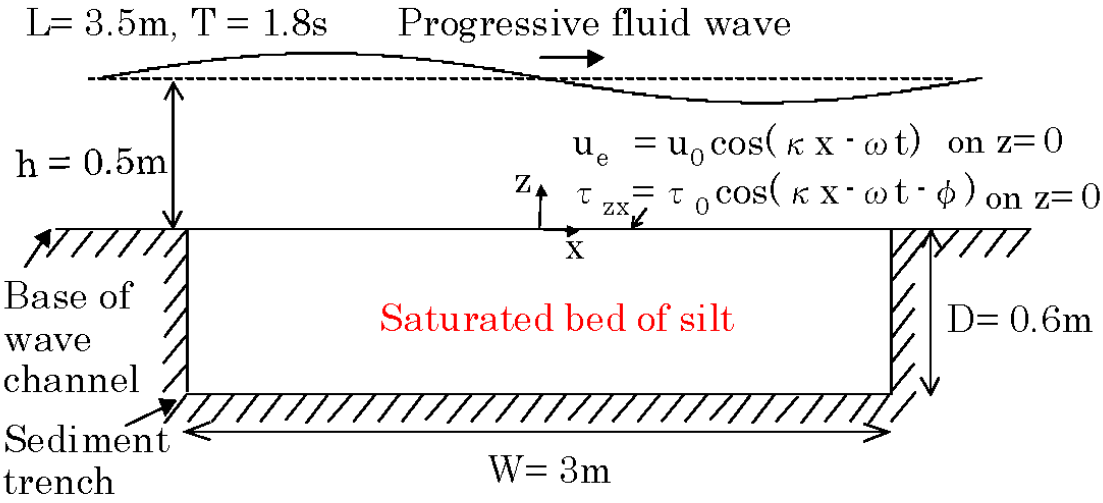

(b) Large scale model by Foda and Tzang(1994)

Fig.3 — Elastoplastic finite element analyses for reproducing the observed wave-induced liquefaction

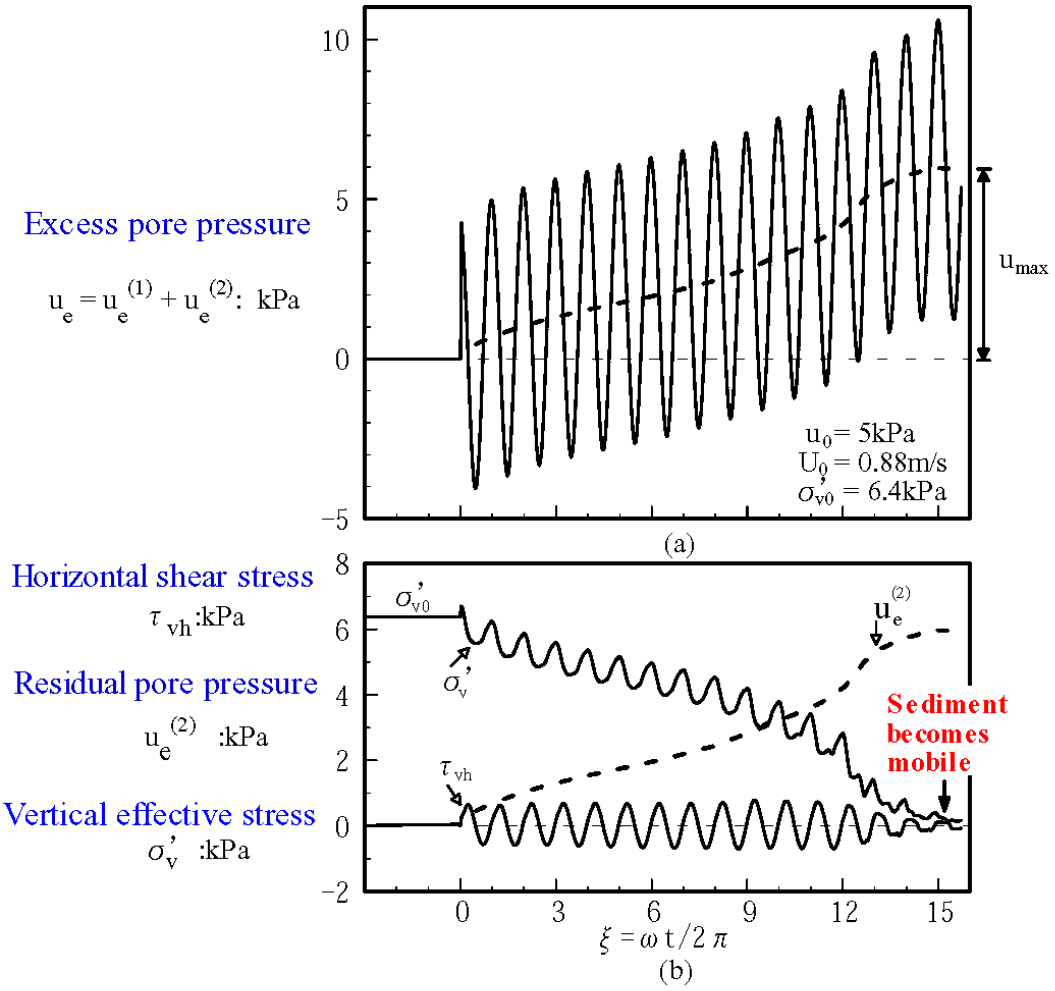

Fig. 4 — Variations with time of τ_{vh}, $u_e^{(2)}$ and σ_v' at the bottom of the mobile layer z = -75cm under waves (S= 0.075, κafw = 0.001, $\Phi = 4.7 \times 10^{-3}$)

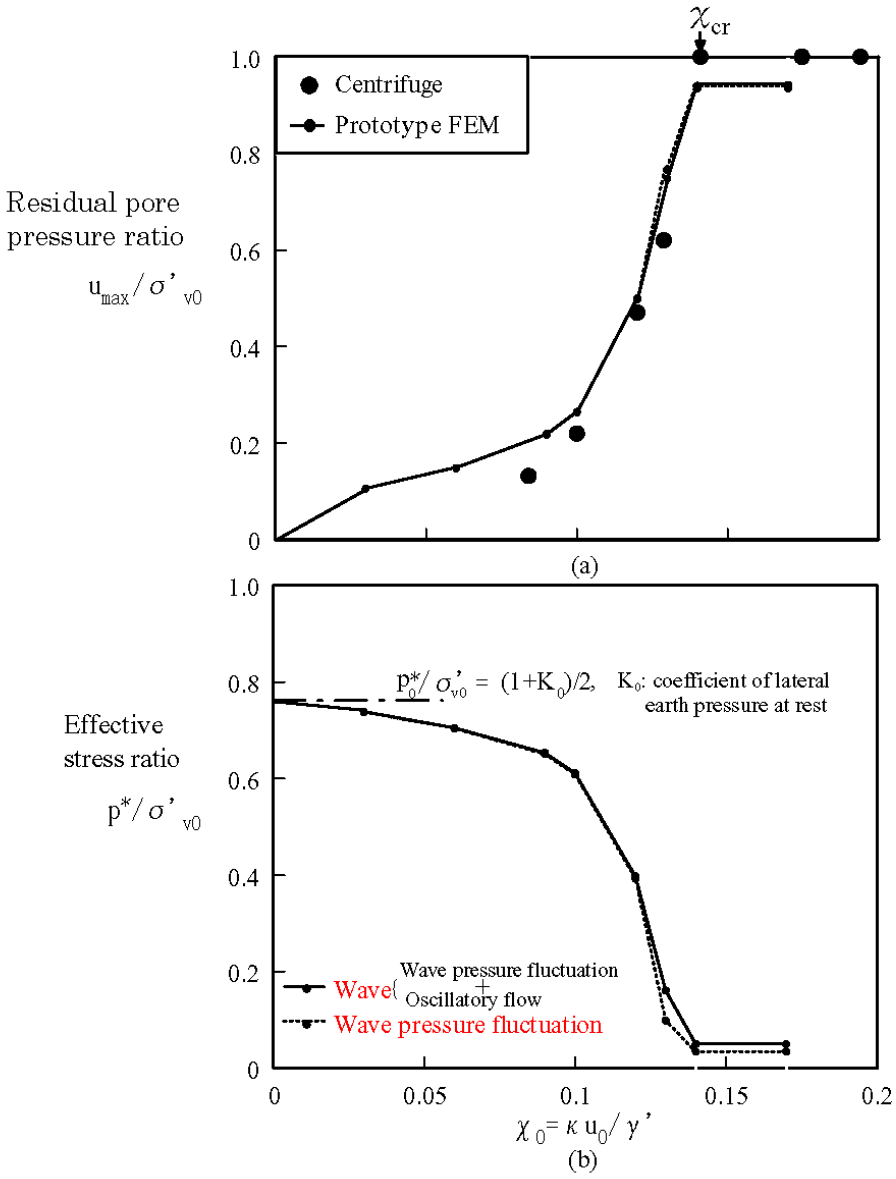

Fig. 5 — Variation with χ_0 of u_{max}/σ'_{v0} and p^*/σ'_{v0} showing the critical cyclic stress ratio for liquefaction to occur

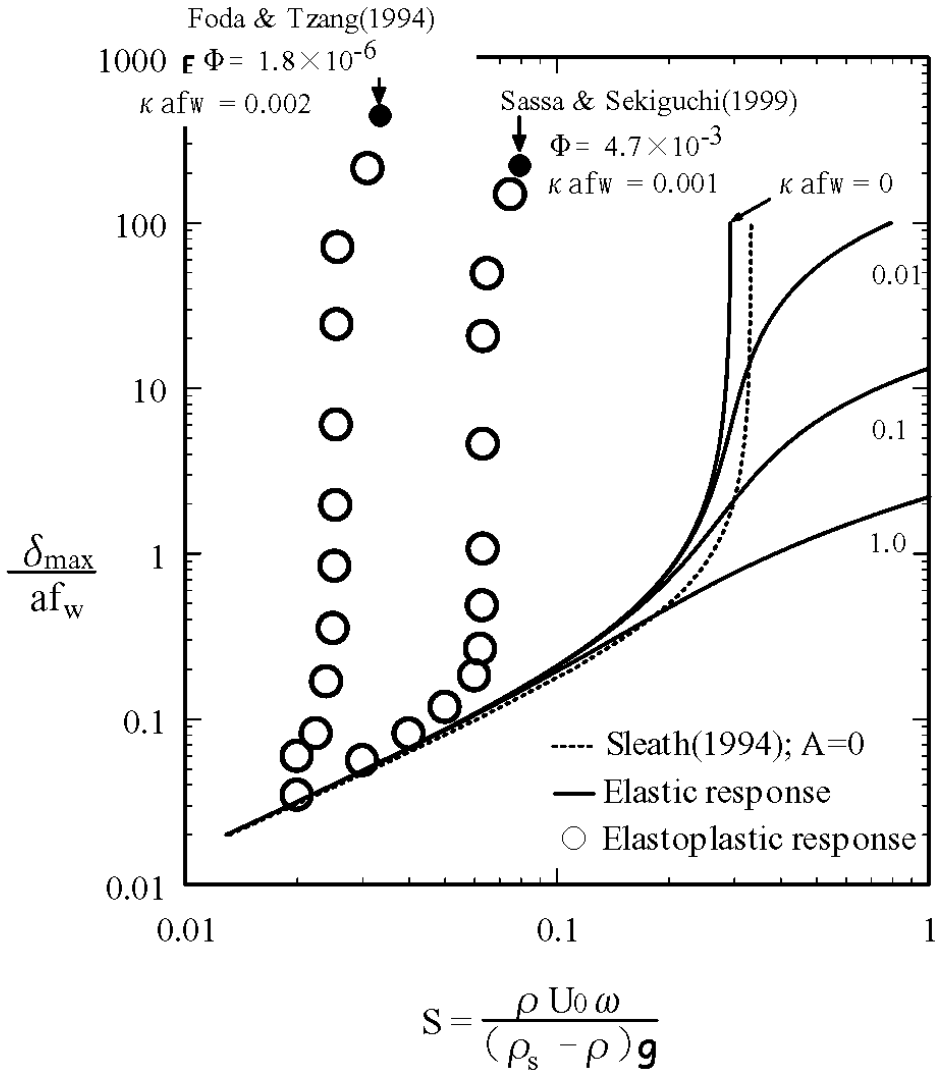

Fig. 6 — Summary plot showing the effect of pore pressure build-up on the maximum thickness of mobile layer under waves